LIMNOLOGY
and
OCEANOGRAPHY

ASLO

Limnol. Oceanogr. 00, 2018, 00–00

doi: 10.1002/lno.10790

Benthic uptake of phytoplankton and ocean-reef exchange of particulate nutrients on a tide-dominated reef

Renee K. Gruber [1,2,3]* **Ryan J. Lowe,** [1,2] **James L. Falter** [1,2]

[1]The Oceans Institute and School of Earth Sciences, University of Western Australia, Crawley, Western Australia, Australia
[2]ARC Centre of Excellence for Coral Reef Studies, University of Western Australia, Crawley, Western Australia, Australia
[3]Australian Institute of Marine Science, Townsville, Queensland, Australia

Abstract

Benthic fluxes of chlorophyll *a* (Chl *a*) and particulate organic carbon (POC) and nitrogen (PON) were quantified on Tallon reef, a strongly tide-dominated (spring range > 8 m) reef located in the Kimberley region of northwestern Australia, over a 2-week period. Extensive hydrodynamic observations were used to construct a reef-scale mass balance to estimate material exchange between the reef and ocean over individual tidal cycles. Additionally, a one-dimensional control volume approach was used to estimate fluxes of Chl *a* in waters traversing the reef platform. Particulate material was delivered to the reef platform in a pulse during flood tide, and benthic uptake of Chl *a* declined to negligible values toward the end of ebb tide. On the scale of tidal cycles, a net uptake of Chl *a* was observed on the reef platform (on average 1.3 mg Chl *a* m^{-2} d^{-1}), which was lower than previous studies of many reef communities. Fluxes showed variability depending on the magnitude of individual tidal cycles, which was likely related to volumes of oceanic Chl *a* inputs. Tallon reef was a net source of detrital POC and PON to the surrounding coastal ocean, with average POC exports ~ 3% of the reef's benthic gross primary production. Seasonal measurements of water quality reported here are among the first records for the coastal Kimberley, and suggest that reefs in the west Kimberley may experience naturally elevated levels of phytoplankton and particulate nutrients, especially during the wet season.

Marine particulate organic matter (POM) is an important component of the coastal nutrient pool that includes bacteria, phytoplankton, zooplankton, and detrital matter (Volkman and Tanoue 2002). POM is a major nutrient source for many reef organisms including active filter-feeders such as sponges (Bell 2008) and passive suspension feeders such as corals (Houlbrèque and Ferrier-Pagès 2009). In oligotrophic reef waters, the smallest fraction of phytoplankton (the picoplankton) generally dominate the pool of "living" POM (Charpy 2005); therefore, most recent studies on reef community grazing have focused on the uptake of small particles (e.g., Ayukai 1995; Patten et al. 2011). It has been suggested that elevated levels of POM may increase reef heterotrophy, especially in low-light environments (Fabricius 2005), but very few studies have quantified reef-scale fluxes of organic particles (e.g., Fabricius and Dommisse 2000; Cuet et al. 2011; Wyatt et al. 2013).

Previous work has demonstrated that reef community grazing rates are a function of both POM concentration and flow conditions, the latter of which enhances rates of particle delivery to the benthos through vertical turbulent convection (Ribes and Atkinson 2007; Jones et al. 2009; Monismith et al. 2010). Thus, measurements of both the oceanic supply of particles to reefs and the local flow conditions are necessary to explain observed rates of community grazing. Many previous studies on particle uptake by benthic communities have been conducted on wave-dominated reef systems where wave-breaking on the forereef drives mainly unidirectional currents across the reef flat (Monismith 2007). The input of oceanic POM to such wave-dominated systems is generally consistent on the scale of days and is controlled by offshore supply and local hydrodynamic conditions (Wyatt et al. 2012). However, there are many other reefs (up to a third worldwide) where the mean tidal range exceeds the local significant wave height and are thus considered to be "tide-dominated" (Lowe and Falter 2015). These reefs experience rapid changes in water depth and flow speed (Lowe et al. 2015) that, in turn, could increase the delivery rate of particle-rich waters to grazing organisms as a function

*Correspondence: r.gruber@aims.gov.au

of the tidal phase. Thus, tide-dominated reefs are expected to show large changes in benthic POM fluxes over a tidal cycle, with maximum rates of uptake occurring when flow velocities and oceanic inputs are greatest.

Controlled flume studies have been important in identifying the roles of grazer assemblage (Yahel et al. 2006) and flow speed (Ribes and Atkinson 2007) on grazing rates, but estimates are mainly relevant for the specific experimental grazing community being examined (Ribes et al. 2005). Methods such as Lagrangian sampling of waters following drogue tracks (Yahel et al. 1998; Cuet et al. 2011) or control volume (CoVo) approaches that utilize continuous velocity measurements and Eulerian sampling to estimate fluxes over a volume of interest (Genin et al. 2009; Monismith et al. 2010) have provided researchers with direct in situ estimates of grazing rates by reef communities; however, only a limited number of these studies have been conducted to date. Indirect estimates of particle uptake rates derived from mass budgets of particulate organic carbon or chlorophyll *a* (Chl *a*) (Ayukai 1995; Cuet et al. 2011) have also been useful, but these techniques have limited applicability and may introduce large errors if local flow conditions are not well-constrained. Although a moderate number of studies have examined in situ grazing by reef communities, no studies have yet addressed the influence of tidal forcing on the supply or uptake rates of phytoplankton or particulate nutrients on reefs.

In this study, we examine the net benthic fluxes of phytoplankton, POC, and PON on a strongly tide-dominated reef. Two complementary approaches were used given the complex and rapidly varying flows of such systems: a one-dimensional control volume and a mass balance. These results will help identify how tidal forcing, the dominant hydrodynamic process for many reefs worldwide, can control inputs of oceanic material to reef communities and can influence benthic fluxes of organic particles within and over tidal cycles. These results will also be compared to rates of reef metabolism to estimate the contribution of reef-scale benthic particle uptake to net community production.

Methods

Field site

The Kimberley region is a remote and near-pristine portion of northwest Australia containing $\sim$ 2000 km^2 of total reef area (Kordi and O'Leary 2016). Its coast is macrotidal with spring tide ranges reaching 12 m (Kowalik 2004), and thus its reef systems are strongly tide-dominated (Lowe and Falter 2015). Tallon Island, located in the Buccaneer Archipelago of the west Kimberley, contains a large (surface area 2.2×10^6 m^2) intertidal fringing reef platform that sits just above mean sea level (+0.25 m Australian height datum [AHD]) and is bounded on its seaward edge by a slightly shallower (+0.35 m AHD) crest (Fig. 1). These features result in strong tidal asymmetry on the reef platform (Lowe et al. 2015), where the ebb phase of the dominant semi-diurnal tide is elongated to $\sim$ 10 h and the flood phase is truncated to $\sim$ 2 h (Fig. 2). Although offshore water levels fall well below the reef platform during ebb tide, reef communities remain submersed through the ebb phase due to the shallower crest and friction from the benthos, with minimum water depths of $\sim$ 0.4 m occurring at the end of the ebb phase (Fig. 2a). Previous studies have addressed the hydrodynamics (Lowe et al. 2015), thermodynamics (Lowe et al. 2016), and community productivity (Gruber et al. 2017) of Tallon reef.

The platform contains two types of benthic community: a seagrass-dominated inner zone and a macroalgae-dominated outer zone that are separated by a zone $\sim$ 200 m wide where the two community types become mixed within a sand and coral rubble substrate (Fig. 1). The inshore seagrass meadow contains *Enhalus acoroides* and *Thalassia hemprichii* growing on sand (Wells et al. 1995), while the macroalgal zone is dominated by the brown macroalgae *Sargassum* spp. growing on lithified reef framework that also contains a diverse assemblage of foliose brown macroalgae, red corallines, and crustose coralline algae. Filter feeding organisms found in the macroalgal-dominated zone include sponges, giant clams (*Tridacna* and *Hippopus* spp.), soft corals, small hard corals (5–10% cover), and likely cryptic filter feeders within the porous reef framework (Richter et al. 2001). Sponges were the main filter feeder found in the seagrass and mixed zones, with a large number of detritivorous sea cucumbers observed at densities of $\sim$ 0.5 individuals m^{-2}, although organism densities were not quantified.

Three field experiments were conducted at Tallon reef with each lasting 1–2 weeks: 05 Oct 2013–20 Oct 2013 (dry season), 04 Feb 2014–09 Feb 2014 (wet season), and 27 Mar 2014–09 Apr 2014 (late wet season) (Table 1). Fixed volumes of water were filtered to determine Chl *a* and particulate nutrient concentrations during all field experiments according to the protocols below. The final field experiment coincided with the detailed hydrodynamic study reported in Lowe et al. (2015). By deploying in situ-calibrated fluorometers and an automated sampler among hydrodynamic instrumentation, we were able to estimate benthic fluxes of POM on the reef platform using two approaches: a one-dimensional control volume technique and a mass balance, as detailed below. Throughout this manuscript we refer to "benthic fluxes" (the "net uptake" or "net release") of Chl *a* and particulate nutrients, rather than "grazing." Due to the rapidly varying flows characteristic of Tallon reef and the design of this study, it was not possible to delineate between rates of grazing by benthic organisms and net deposition (or resuspension). However, we will demonstrate that grazing is likely the dominant process driving observed benthic fluxes, especially for small particles (*see* "Discussion" section).

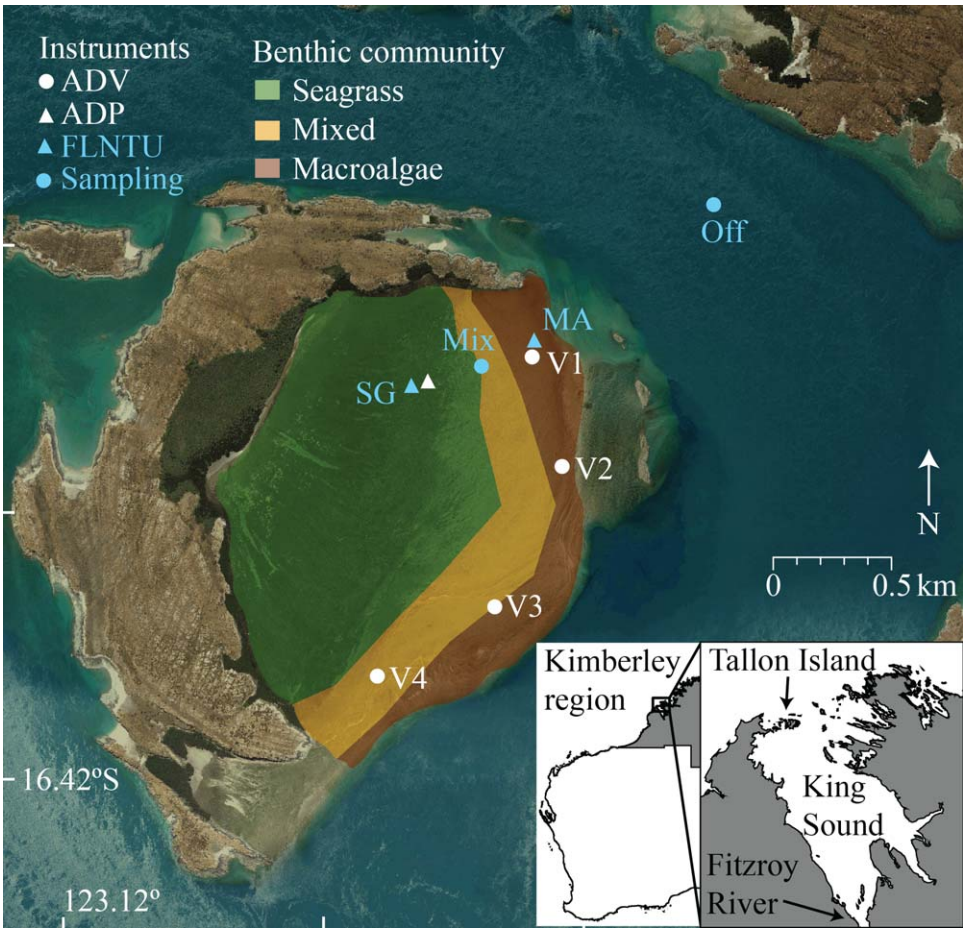

Fig. 1. Deployment locations of instrumentation and hand sampling locations on Tallon reef platform. Inset shows Tallon Island location in the west Kimberley region of Australia. ADV refers to acoustic Doppler velocimeters, ADP refers to acoustic Doppler profiler, and FLNTU refers to fluorometers.

Water sampling

Extensive water sampling was conducted during each field experiment to determine concentrations of Chl *a* and particulate organic nutrients offshore and on the reef. The majority of our sampling efforts were conducted at four fixed (Eulerian) stations: the channel adjacent to the reef ("Off"), and on the reef platform in the macroalgal-dominated zone ("MA"), the mixed zone ("Mix"), and the seagrass-dominated zone ("SG") (Fig. 1). Offshore samples were collected by boat at roughly 1 h intervals on the days when water sampling occurred (Table 1). Samples from the reef were collected on foot during the middle to end of ebb tide (6–12 h after reef flooding, Fig. 2) and by boat when water levels were higher (1–4 h after reef flooding). Sampling by boat or on foot was not possible during peak flood and ebb periods (0–1 h and 4–6 h after reef flooding, respectively, Fig. 2) due to the hazardous flow conditions on the reef. Thus, an ISCO automated water sampler (Teledyne Isco) was placed on a 4 m high scaffolding at Mix (Fig. 1) during the Apr field experiment and sampled hourly during the first few hours after reef flooding (Table 1). Lagrangian sampling of water masses traversing the reef was also conducted during the Oct field experiment. A small neutrally-buoyant drogue (mandarin) with GPS tracker attached was released at SG or MA ($n = 4$ for each) and allowed to drift for 30 min; wind speeds were generally slow (< 4 m s^{-1}) during the experiment (Gruber et al. 2017) so drogues closely followed the water mass of interest. Water samples were collected at the start and end locations of each drift (Table 1). The drogue velocities were compared when they passed nearby fixed hydrodynamic instruments (see below) to validate the flow estimates obtained by the drogues. Sampling for Chl *a* and all suspended particulates was done in duplicate, and values presented are the mean of duplicates.

Water samples for analysis of Chl *a* concentration were collected in 2 L plastic bottles and filtered under vacuum onto 47 mm (pore size 0.7 μm) filters (Whatman GF/F) within 1 h of collection. The concentration of the large size-fraction Chl *a* (> 5 μm) was determined by filtration through 47 mm (pore size 5 μm) polycarbonate filters (Nuclepore). Filters were folded in aluminum foil and placed on ice until return to the field station where they were frozen until analysis. Water samples for analysis of POC/PON and particulate

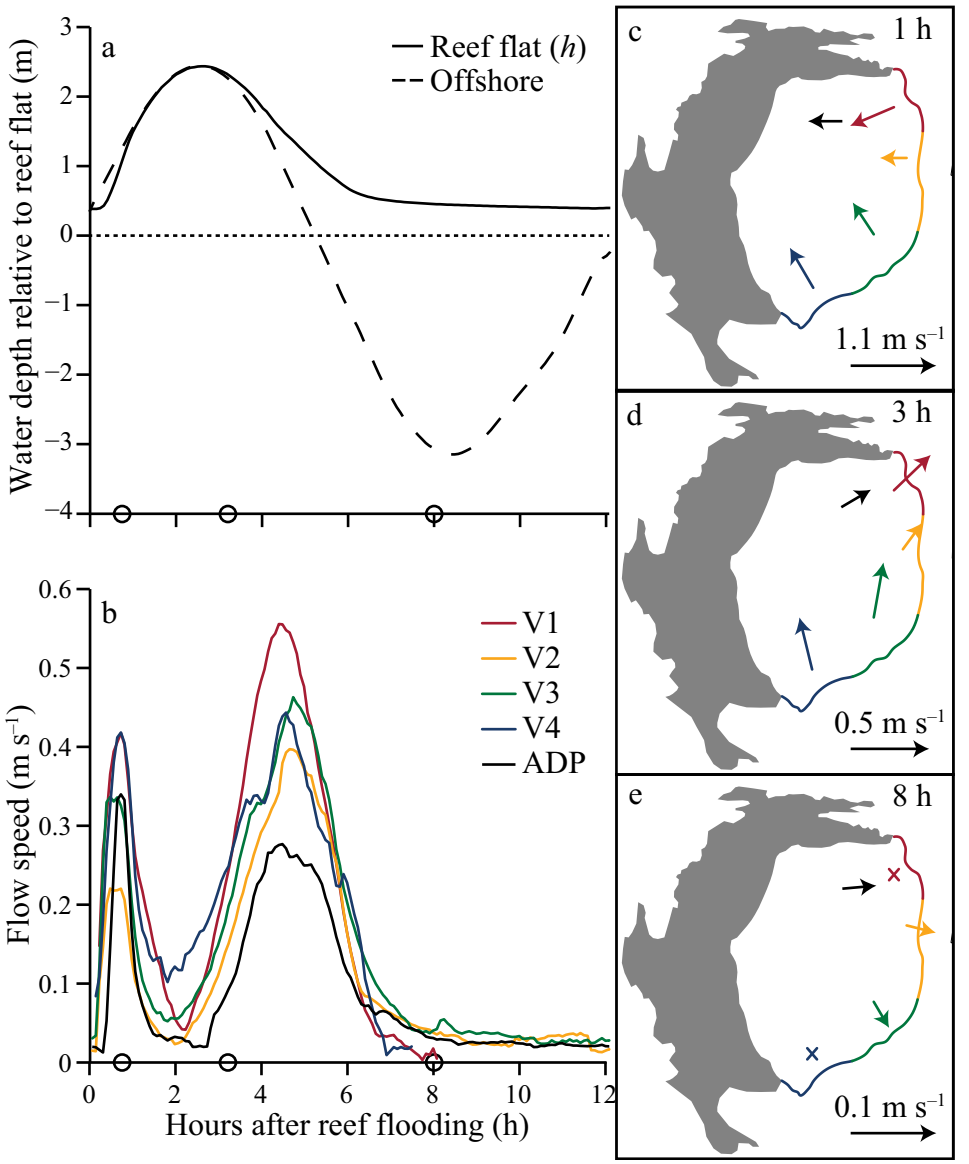

Fig. 2. Tidal phase-averaged hydrodynamic conditions on Tallon Reef including (**a**) water depth at SG (*h*) and offshore; (**b**) current speed at five hydrodynamic instruments (V1–V4 are acoustic Doppler velocimeters and ADP is an acoustic Doppler profiler); and current vectors from (**c**) flood tide, (**d**) start of ebb tide, and (**e**) middle of ebb tide. All values are means from a full spring-neap cycle. Note scale changes on current vectors to emphasize flow patterns. Crosses indicate periods when water depth was too low to measure flow. Length of reef crest (l_i) used for discharge estimates (*see* "Methods" section) is colored to correspond with associated hydrodynamic instrumentation.

phosphorus (PP) were filtered onto 25 mm GF/Fs that had been pre-combusted (4 h at 550°C). The volume filtered was 0.5–2 L, or when sufficient material was collected on each filter. Filters were then rinsed with a small amount (5–10 mL) of ultrapure water, dried under gentle vacuum, placed in pre-combusted aluminum foil packets, and stored frozen until analysis.

All laboratory analyses were conducted within a few weeks of returning from the field. Filters for Chl *a* analysis were placed in 90% acetone, sonicated, and allowed to extract overnight at 4°C. The following day, samples were centrifuged and the supernatant was read on a fluorometer (Turner Designs Trilogy) for total Chl *a*. Samples were then acidified with 0.1N hydrochloric acid for determination of phaeophytin *a* and Chl *a* correction (Arar and Collins 1997). A Shimadzu TOC-V carbon analyzer fitted with solid sample combustion (SSM-5000A) and total nitrogen units was used to measure POC/PON content; filters were acidified pre-combustion to remove inorganic carbonates. A hot acid digestion in 5% persulfate was performed on filters for PP analysis (Menzel and Corwin 1965), and the resulting concentration of liberated phosphate was determined spectrophotometrically (Parsons et al. 1984) with a Shimadzu UV-1601.

Table 1. Number of duplicate Chl *a* samples taken each field experiment at each site, including during Lagrangian drifts and large (> 5 μm) Chl *a* fractions. Number of duplicate particulate organic carbon (POC), nitrogen (PON), and phosphorus (PP) samples are also indicated. Tide stages (ebb, flood) refer to tides on the reef platform and hyphens (-) indicate no samples available.

			Chl *a*					
Dates	**Season**	**Site**	**Ebb**	**Flood**	**Drifts**	**< 5 μm**	**POC/PON**	**PP**
05 Oct 2013–20 Oct 2013	Dry	Off	9	7	-	9	4	6
		MA	22*	10	8	12	-	3
		SG	6*	10	8	4	-	-
04 Feb 2014–09 Feb 2014	Wet	Off	14	3	-	-	12	12
		MA	14*	-	-	-	11	11
		SG	13*	-	-	-	10	10
27 Mar 2014–09 Apr 2014	Late Wet	Off	13	11	-	-	3	-
		MA	7*	-	-	-	2	-
		Mix	9	10	-	-	14	5
		SG	6*	-	-	-	-	-

* Indicates samples from the final 6 h of ebb tide.

Control volume approach

A one-dimensional control volume (CoVo) approach was used to estimate the net benthic flux of Chl *a* during the Apr field experiment. This method utilizes flow velocity and modified Eulerian sampling of Chl *a* at upstream and downstream points, and we have already used a similar approach to estimate net community productivity on Tallon reef (Gruber et al. 2017). Current velocity (u) and water depth (h) were recorded at 1 Hz by a bottom-mounted acoustic Doppler current profiler (Nortek Aquadopp HR AS) with 0.03 m bin size, located near SG (Fig. 1). Toward the end of ebb tide, the water depth reached a minimum on the reef platform ($h \approx 0.4$ m, Fig. 2), and in the rare instances (5% of the total field study) where water depth encroached on instrument blanking distance, the flow speed was estimated from drifter releases (Gruber et al. 2017). Tidal phase-averaging is used throughout this manuscript to present patterns in hydrodynamic and other continuous data related to the phase of tide. Phase-averages are ensemble averages of a given variable at each point in a tidal cycle (e.g., mean of all values measured at high tide).

Fluorometers (Wetlabs FLNTUSB) deployed at MA and SG (Fig. 1) burst-sampled at 1 Hz every 5 min, yielding data over 17 complete tidal cycles. Fluorometers were placed together for 30 min periods during the start, middle, and end of the field experiment to check for drift, which was negligible. Instrument output was bin-averaged at 5 min intervals and calibrated to in situ conditions using regressions with Chl *a* samples taken during the experiment ($R^2 = 0.74$, $p < 0.001$); fluorometers slightly underestimated Chl *a* by $\sim$ 25% on average and were therefore calibrated to in situ Chl *a* concentrations. Water samples were collected over the wide ranges of irradiance and temperature that naturally occurred on the reef platform, so we are confident that the fluorometers provided a close approximation of in situ Chl *a* concentrations.

During each 10 h ebb tide, water drained off the northern portion of the reef platform in the northeasterly direction ($80° \pm 30°$, mean $\pm$ standard deviation; Fig. 2d,e), aligned with the instrument transect. Depth-averaged flow speed in the direction of the instrument transect (u_x) was bin-averaged at 5 min intervals and used to estimate transport q_x as

$$q_x = u_x h, \tag{1}$$

assuming horizontal dispersion was negligible. The benthic flux of Chl *a* ($J^{CoVo}_{Chl\,a}$ in mg Chl *a* m^{-2} h^{-1}) was estimated as (Genin et al. 2009)

$$-J^{CoVo}_{Chl\,a} = \overline{h}\frac{d\overline{C}}{dt} + q_x\frac{(C_{MA} - C_{SG})}{dx}, \tag{2}$$

where C_{MA} and C_{SG} are the Chl *a* concentrations at MA and SG, respectively, and $\overline{C}$ is the mean of both. The transect length dx was 540 m and $\overline{h}$ represents mean water depth at MA and SG. Note that a sign convention is assumed where positive $J^{CoVo}_{Chl\,a}$ indicates net uptake of Chl *a* by the benthos while negative values indicate net release to the water column. The first term on the right side of Eq. 2 represents the mean local benthic flux of Chl *a* (i.e., uptake or release in the vicinity of the loggers), while the second term refers to the uptake or release of Chl *a* during advection between loggers. The local term was bin-averaged into 30-min increments, beginning at peak high tide. As flow speeds change throughout ebb tide, a varying averaging interval was used for the advective term; estimates were bin-averaged based on transit time between SG and MA and then linearly interpolated onto a common 30 min interval (Gruber et al. 2017). This formulation assumes that

phytoplankton growth and pelagic grazing have a similar (small) magnitude on the timescale of hours (Genin et al. 2009). The CoVo approach was relevant for ebb tide periods (~ 10 h each semidiurnal tidal cycle) when flow vectors were aligned with the instrument transect. Lagrangian measurements following drifters provided an independent estimate of benthic Chl *a* flux during ebb tides. Fluxes (in mg Chl *a* m^{-2} h^{-1}) were estimated as

$$J_{\mathrm{Chl}\,a}^{\mathrm{Drift}} = \overline{h_{\mathrm{drift}}}\Delta C/\Delta t, \tag{3}$$

where ΔC was the change in Chl *a* concentration from water samples taken at the start and end of the drift, Δt was drift time, and $\overline{h_{\mathrm{drift}}}$ was the mean water depth along the drifter track.

Reef-scale mass balance

Although useful for determining benthic Chl *a* fluxes during ebb tides, the CoVo approach could not account for fluxes during flood tides, when flow direction changed rapidly, the flows were not aligned with the instrument transect, and resuspension obscured spatial Chl *a* gradients (*see* "Discussion" section). In order to understand how representative the CoVo estimates were during a full tidal cycle and at the larger reef platform scale, we utilized a second approach: a mass balance that estimated Chl *a* exchange across the reef crest. A similar approach was used to construct a reef-scale heat budget for Tallon reef (Lowe et al. 2016). Flow velocities and water depths were recorded at 2 Hz by four upward-looking acoustic Doppler velocimeters (Nortek Vector) evenly spaced along the reef crest (V1-4, Fig. 1). Raw data were despiked (Goring and Nikora 2002), filtered for instances when water depth approached the sampling volume (0.4 m above the bed), and averaged at 5 min intervals. Cross-shore transport (q_i, where $i = 1 : 4$ corresponding to instruments V1-4) was defined for each instrument as the transport component normal to the reef crest, with the convention that onshore flow was positive. Low water depth affected instruments V1 and V4 toward the end of ebb tide (Fig. 2b), when flows were slow (< 0.05 m s^{-1}); for these instances, q_1 was assumed to equal q_x (i.e., transport was conserved), and q_4 was assumed to be similar in magnitude to all other q_i. The integrated discharge across each of the four segments of reef crest Q_i (in m^3 s^{-1}) was estimated as

$$Q_i = q_i l_i, \tag{4}$$

where l_i is the length of crest represented by each of the four cross-reef transport terms (shown in color Fig. 2c–e). Total discharge in the onshore direction Q_{in} was the sum of all positive Q_i each time step, while discharge offshore Q_{out} was the sum of all negative Q_i. In order to estimate the rate of phytoplankton import into the reef system, we assumed water entering the reef at flood tide (Q_{in}) had a constant Chl *a* concentration equal to the mean at Off during the Apr field experiment (0.60 μg L^{-1}, Fig. 3a). Offshore Chl *a* concentrations were relatively constant (standard error of the mean = 0.04 μg L^{-1}), but uncertainty was nonetheless incorporated into error estimates (described below). The rate of Chl *a* import from offshore waters (F_{in}, in mg Chl *a* s^{-1}) was estimated each time step as

$$F_{\mathrm{in}} = Q_{\mathrm{in}} C_{\mathrm{o}}, \tag{5}$$

where C_{o} was offshore Chl *a* concentration. We assumed that water exiting the reef during ebb tide (Q_{out}) would have Chl *a* concentrations equivalent to those measured at MA (C_{MA}), the fluorometer closest to the reef crest. This assumption was based on the observations that: (1) during the early portion of ebb tide (when the majority of Q_{out} occurs), offshore discharge mainly crosses l_1, the boundary associated with C_{MA} (Fig. 2d); and (2) toward the end of ebb tide (when Q_{out} is very low), all flow streamlines (Fig. 2e) pass over benthic communities of similar composition (Fig. 1). Despite several assumptions associated with the mass balance, we will show that estimates from this method compared well to estimates made using the entirely different CoVo approach (*see* "Results" section), which gives us confidence that these assumptions are reasonable.

The rate of Chl *a* export from the reef platform (F_{out}) during each time step was then estimated as

$$F_{\mathrm{out}} = Q_{\mathrm{out}} C_{\mathrm{MA}}, \tag{6}$$

and the net rate (F_{net}) of Chl *a* import or export each time step was then

$$F_{\mathrm{net}} = F_{\mathrm{in}} + F_{\mathrm{out}}. \tag{7}$$

In order to represent the overall balance between oceanic inputs and off-reef exports, estimates of F_{net} were integrated over each semidiurnal tidal cycle, where F_{cyc} was the sum of all F_{net} occurring from the start of flood tide (zero hours after flooding) to the end of ebb tide (~ 12.4 h after reef flooding) for each of the 17 tidal cycles. We then calculated a mean net benthic flux $J_{\mathrm{Chl}\,a}^{\mathrm{MB}}$ (in mg Chl *a* m^{-2} d^{-1}) for each tidal cycle as

$$J_{\mathrm{Chl}\,a}^{\mathrm{MB}} = F_{\mathrm{cyc}}/\left(A_{\mathrm{reef}} t_{\mathrm{cyc}}\right), \tag{8}$$

where t_{cyc} is the tidal cycle length (in days), and A_{reef} is the reef platform surface area. Positive values indicate net uptake of Chl *a* on the reef, while negative values indicate net Chl *a* release offshore. In order to compare benthic fluxes estimated with the CoVo and mass balance approaches, $\overline{J_{\mathrm{Chl}\,a}^{\mathrm{CoVo}}}$ (in mg Chl *a* m^{-2} d^{-1}) was calculated as the mean of all $J_{\mathrm{Chl}\,a}^{\mathrm{CoVo}}$ during each tidal cycle.

The input of phytoplankton-derived particulate nutrients on the reef was estimated using significant linear relationships ($p < 0.01$) between concentrations (in μg L^{-1}) of POC and Chl *a* ($R^2 = 0.61$) and PON and Chl *a* ($R^2 = 0.80$) during the Apr field experiment. The flux of phytoplankton-derived POC with each tidal cycle (POC_p) could then be estimated

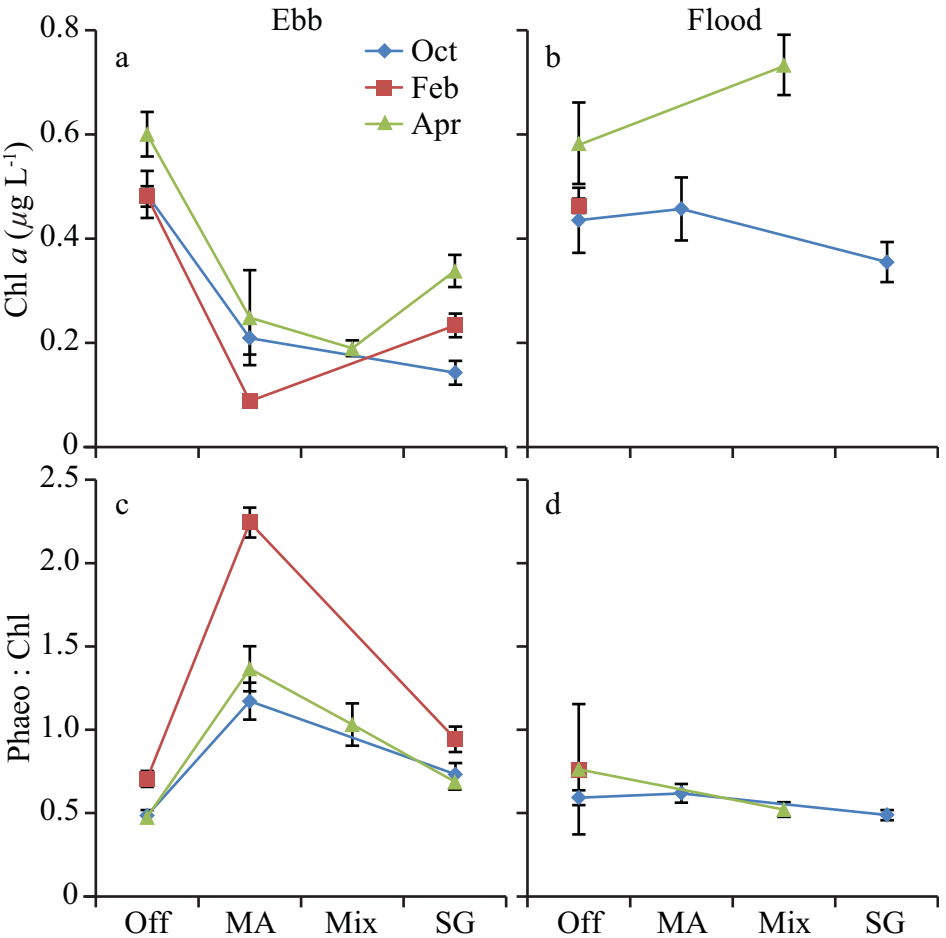

Fig. 3. Mean (± SE) Chl *a* (**a**, **b**) and ratio of phaeopigments : Chl *a* (**c**, **d**) from water samples at offshore (Off) and reef stations [macroalgal (MA), mixed (Mix), and seagrass (SG) dominated zones] during all field experiments. Samples are categorized as taken during flood tide or during ebb tide (final 6 h) on the reef platform. The number of samples represented by each mean is shown in Table 1. [Color figure can be viewed at wileyonlinelibrary.com]

as the product of the regression coefficient, 36.7 ± 21.8 (mean ± 95% confidence interval), and $J^{MB}_{Chl\,a}$. Note that this empirically derived conversion factor is very similar to the carbon : Chl *a* ratio of 30 : 1 commonly assumed in phytoplankton studies (Cloern et al. 1995). The flux of phytoplankton-derived PON (PON_p) could be similarly estimated as the product of 10.10 ± 3.78 and $J^{MB}_{Chl\,a}$. This empirically derived ratio of nitrogen : Chl *a* is at the upper end of the range (1.70–14.7) reported in previous studies (Yentsch and Vaccaro 1958; Wyatt et al. 2010) and implies a C : N ratio below Redfield, yet within the range found in natural populations (Geider and La Roche 2002).

Using a mass balance approach similar to the above for Chl *a* (Eqs. 4–7), benthic fluxes of total POC and PON were estimated over a mean tidal cycle using phase-averaged versions of discharges Q_{in} and Q_{out}. Water sampling on the reef platform occurred over multiple tidal cycles, so POC and PON concentrations, while variable, could be considered representative of a mean tidal cycle. Oceanic inputs of POC and PON during flood tide were assumed to be at the same concentrations as the mean values at Off (Eq. 5). Significant nonlinear relationships commonly observed in reef particulate uptake studies (Ribes et al. 2003, 2005), were fit to POC and PON measurements ($R^2 = 0.46$ and 0.57, respectively) to estimate concentrations over a full ebb tide at Mix (*see* "Results" section), which was assumed to be similar to POC and PON in water exiting the reef platform (Eq. 6). Finally, mean benthic fluxes of total POC and PON were calculated as the balance between oceanic inputs and off-reef export during ebb tide (Eqs. 7, 8).

Statistics and error propagation

Significant differences among means of water quality variables were assessed with one-way ANOVAs using SAS statistical software (v9.4). The assumption of homoscedasticity was met with Levene's test, and normality of residuals was assessed both visually and through the Shapiro–Wilk normality test. Tukey–Kramer adjusted least-squared

means were calculated, and all pair-wise comparisons were computed. In cases where data required transformation to meet assumptions, uncertainty around the mean was represented by back-transformed 95% confidence limits. Uncertainties in estimates of $J^{CoVo}_{Chl\,a}$ and $J^{MB}_{Chl\,a}$ were calculated via Monte Carlo simulation ($n = 10{,}000$) where input variances were drawn from bin-averaged data (Lehrter and Cebrian 2010).

Results

Chl *a* and particulate nutrients

Offshore Chl *a* concentrations were similar between the first two field experiments during the dry and early wet seasons (~ 0.45 μg L^{-1}), and were elevated by the end of the wet season in Apr (0.60 μg L^{-1}); offshore Chl *a* values were similar during flood and ebb tidal phases during all field experiments (Fig. 3a,b). Ratios of phaeophytin to Chl *a* were ~ 0.6 for offshore waters (Fig. 3c,d). Size-fractionated Chl *a* values showed that the offshore phytoplankton pool contained comparable amounts of both "small" (< 5 μm) and "large" (> 5 μm) cell sizes (Fig. 4a,b). The large fraction also tended to contain comparatively more degraded Chl *a* than the small fraction, with phaeo : chl ratios of 0.9 and 0.3, respectively (Fig. 4c,d). Unlike Chl *a*, offshore particulate nutrient concentrations were lowest during the final field experiment; the low values for ratios of POC : Chl *a* and PON : Chl *a* suggested that phytoplankton comprised a larger proportion of total POC and PON at the end of the wet season than during other field experiments (Table 2).

In contrast to offshore waters, Chl *a* and particulate nutrient concentrations on the reef platform were highly dependent on the tidal phase. For samples taken around high tide, Chl *a* and phaeo : chl were similar to offshore measurements (Fig. 3b,d). During ebb tide, however, Chl *a* on the reef platform declined, reaching less than half of offshore levels by the end (final 6 h) of ebb tide (Fig. 3a); this trend was observed during all three field experiments. Ratios of phaeo : chl on the reef increased by the end of ebb tide, up to a factor of 3 during the Feb field experiment; in all field experiments, maximum values of phaeo : chl were found at MA (Fig. 3c). Both large (> 5 μm) and small (< 5 μm) size fractions of Chl *a* were significantly reduced ($p < 0.003$) by the end of ebb tide on the reef relative to offshore waters (Fig. 4a,b). Ratios of phaeo : chl were also significantly elevated ($p < 0.005$) in both small (Fig. 4c) and large (Fig. 4d) size fractions on the reef relative to offshore.

Toward the end of ebb tide on the reef platform (final 6 h of the ~ 10 h of ebb tide), suspended particulate nutrient concentrations on the reef were depressed by up to ~ 50% relative to offshore values (Table 2). Concentrations of POC, PON, and PP were consistently lowest at MA (compared to Off and SG) during each field experiment. The stoichiometry of particulate nutrients differed between the reef and

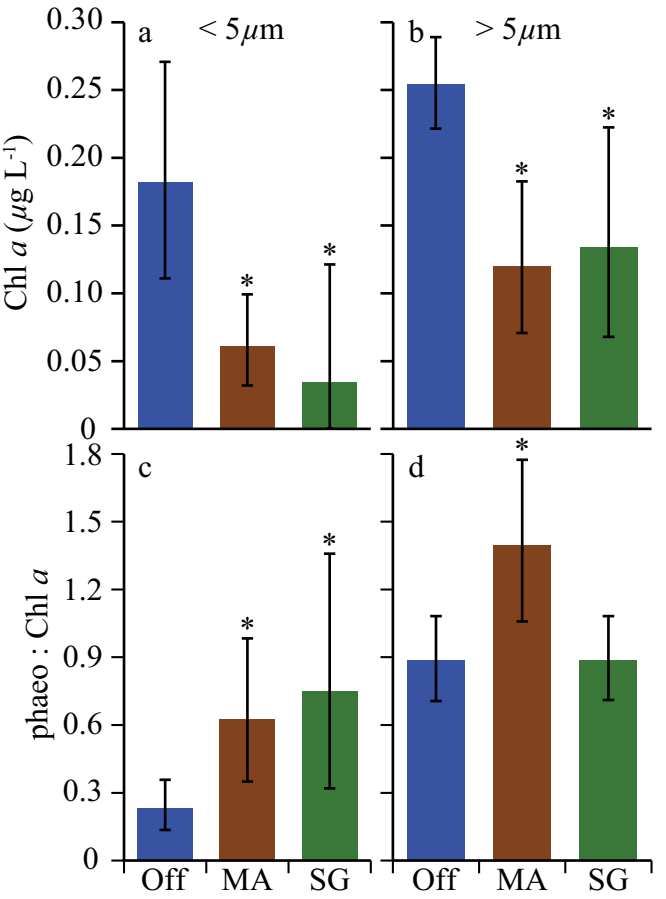

Fig. 4. Mean (with 95% confidence limits) Chl *a* concentration (**a**, **b**) and ratio of phaeophytin : Chl *a* (**c**, **d**) from water samples in small (< 5 μm) and large (> 5 μm) fractions at offshore (Off) and reef stations [macroalgal (MA) and seagrass (SG) dominated zones]. All samples taken during the Oct field experiment during final 6 h of ebb tide on the reef (Table 1). Asterisks (*) denote means which are significantly different ($p < 0.05$) to offshore means. [Color figure can be viewed at wileyonlinelibrary.com]

offshore waters (Table 2), with elevated PON : PP and POC : PP observed at MA and SG. Ratios of particulate nutrients to Chl *a* showed that Chl *a* declined relative to total POC, PON, and PP on the reef; highest ratios of POC : Chl *a* and PON : Chl *a* were observed in the MA and Mix zones during the Feb and Apr field experiments (Table 2).

Continuous Chl *a* measurements on the reef showed distinct features related to phases in the tidal cycle (Fig. 5); Chl *a* concentrations rose sharply during flood tide (0–3 h after reef flooding) when offshore waters inundated the reef platform. During each tidal cycle, maximum Chl *a* concentrations occurred in conjunction with high flow velocities produced by each peak flood and peak ebb (~ 0–1.5 h and 4–6 h after reef flooding, respectively), and could reach ~ 1.0 μg L^{-1} during spring tides (Fig. 5b,c). Chl *a* concentrations declined as water levels on the reef platform became low, and Chl *a* generally remained low for the remainder of ebb tide (final 6 h), as was independently observed in the

Table 2. Summary of mean (*SD*) concentrations and stoichiometry of particulate organic carbon (POC), nitrogen (PON), and phosphorus (PP) from all field experiments. Reef zone [macroalgal (MA), mixed (Mix), and seagrass (SG)] values are from final 6 h of ebb tide, and offshore (Off) values are from all stages of the tide. Number of samples represented by each mean are shown in Table 1 and hyphens (-) indicate no data available.

		Concentration (μM)						Ratio (μg μg^{-1})		
		POC	PON	PP	POC : PON	PON : PP	POC : PP	POC : Chl *a*	PON : Chl *a*	PP : Chl *a*
Oct 2013	Off*	14.6 (*3.1*)	2.77 (*0.61*)	0.068 (*0.019*)	5.25 (*1.61*)	40.9 (*14.6*)	214 (*76*)	388 (*154*)	86 (*34*)	4.7 (*2.0*)
	MA	-	-	0.027 (*0.008*)	-	-	-	-	-	4.0 (*3.1*)
	SG	-	-	-	-	-	-	-	-	-
Feb 2014	Off*	14.6 (*5.9*)	1.71 (*0.25*)	0.090 (*0.029*)	8.52 (*3.66*)	19.0 (*6.7*)	162 (*83*)	373 (*156*)	51 (*9*)	6.0 (*2.0*)
	MA	9.2 (*3.7*)	0.95 (*0.39*)	0.030 (*0.024*)	9.74 (*5.64*)	31.7 (*28.6*)	309 (*277*)	1258 (*562*)	151 (*69*)	10.5 (*8.7*)
	SG	12.3 (*4.7*)	1.19 (*0.21*)	0.039 (*0.015*)	10.38 (*4.40*)	30.5 (*12.7*)	317 (*169*)	632 (*329*)	71 (*28*)	5.2 (*2.7*)
Apr 2014	Off*	6.5 (*1.3*)	1.10 (*0.22*)	-	5.88 (*1.63*)	-	-	130 (*50*)	26 (*9.9*)	-
	MA	3.7 (*1.3*)	0.49 (*0.22*)	-	7.55 (*4.21*)	-	-	280 (*115*)	43 (*22*)	-
	Mix	7.2 (*2.5*)	0.99 (*0.27*)	0.038 (*0.003*)	7.32 (*3.21*)	25.9 (*7.3*)	190 (*67*)	460 (*191*)	73 (*26*)	6.2 (*1.6*)
	SG	-	-	-	-	-	-	-	-	-

* Samples are from all stages of tide.

water samples (Fig. 3a). Chl *a* at MA was stable $\sim$ 0.1–0.2 μg L^{-1} during this late ebb tide period (Fig. 5b) while concentrations were slightly higher ($\sim$ 0.3–0.4 μg L^{-1}) and more variable at SG (Fig. 5c), although this elevation occurred during daytime periods only.

Benthic Chl *a* fluxes

Benthic fluxes of Chl *a* estimated using the control volume approach ($J^{\mathrm{CoVo}}_{\mathrm{Chl}\,a}$) displayed rapid variations during the early portion of ebb tide, 3–6 h after reef flooding (Fig. 6). A net release of Chl *a* into the water column ($J^{\mathrm{CoVo}}_{\mathrm{Chl}\,a} < 0$) occurred during peak ebb (4 h after reef flooding), which coincided with high flow velocities (Fig. 5). Net uptake of Chl *a* ($J^{\mathrm{CoVo}}_{\mathrm{Chl}\,a} > 0$) occurred during the rest of ebb tide, reaching a maximum 6 h after reef flooding, and tapering to zero by the end of ebb tide (Fig. 6). The Lagrangian estimates of the benthic fluxes from drifter releases at MA closely matched the tidal phase-average of $J^{\mathrm{CoVo}}_{\mathrm{Chl}\,a}$; whereas $J^{\mathrm{Drift}}_{\mathrm{Chl}\,a}$ from the seagrass zone was negligible (Fig. 6).

The flow discharges on and off the reef platform were approximately "balanced" (i.e., water volumes from flood and ebb tides were equal for each tidal cycle), with residual errors of less than 5%. The fact that our water mass balance was approximately "closed" also gave us confidence that this approach could be used to estimate the net uptake or release of POM over an entire tidal cycle. Tidal phase-averaged plots of discharge showed that oceanic inputs (Q_{in}) peaked during flood tide and continued for $\sim$ 3 h of ebb tide (Fig. 7a), due to on-reef flows along the reef platform's southern boundary (Fig. 2d). The majority of off-reef discharge (Q_{out}) occurred at the beginning of ebb tide, 3–6 h after reef flooding, with negligible discharge during the final 6 h of ebb tide. Net transfer of Chl *a* onto the reef ($F_{\mathrm{net}} > 0$) was greatest during peak flood (Fig. 7b). During the beginning of ebb tide (3–6 h after reef flooding), Chl *a* inputs from Q_{in} (Fig. 7a) partially balanced the large Chl *a* exports due to high Chl *a* concentrations in Q_{out} (Fig. 5b). Transport of Chl *a* off the reef platform ($F_{\mathrm{net}} < 0$) became negligible during the final 6 h of ebb tide (Fig. 7b). Positive values of $J^{\mathrm{MB}}_{\mathrm{Chl}\,a}$ indicated net uptake of Chl *a* over each tidal cycle, suggesting that the reef was generally a sink for suspended Chl *a*, although estimates of $J^{\mathrm{MB}}_{\mathrm{Chl}\,a}$ for some tidal cycles were not significantly different to zero (Fig. 8). Large variability in $J^{\mathrm{MB}}_{\mathrm{Chl}\,a}$ between tidal cycles was evident, and $J^{\mathrm{MB}}_{\mathrm{Chl}\,a}$ appeared to have a long-term periodicity on the order of weeks (Fig. 8).

Overall mean benthic fluxes of Chl *a* estimated from the mass balance and CoVo (means of $J^{\mathrm{MB}}_{\mathrm{Chl}\,a}$ and $\overline{J^{\mathrm{CoVo}}_{\mathrm{Chl}\,a}}$, respectively) were similar despite being made on entirely different spatial and temporal scales (Table 3). These estimates demonstrate that Tallon reef platform was a net sink to suspended Chl *a* during the Apr field experiment. For further discussion, we will focus on mass balance estimates of Chl *a* flux ($J^{\mathrm{MB}}_{\mathrm{Chl}\,a}$) since these account for processes occurring over the entire tidal cycle, rather than only ebb tide.

Benthic fluxes of total POC and PON

Measurements of POC and PON concentration occurred over multiple tidal cycles; therefore, exponential decay relationships (*see* "Methods" section) represented phase-averaged particulate concentrations at Mix during the Apr field study (Fig. 9). By using a mass balance approach similar to that of Chl *a*, we were further able to estimate mean fluxes of total POC and PON on the reef platform (Table 4). Phytoplankton-derived particulate nutrients ($\mathrm{POC_p}$ and $\mathrm{PON_p}$) that were retained on the reef represented $\sim$ 7% and $\sim$ 10%, respectively, of the total POC and PON inputs during each tidal cycle; however, we measured the net release of

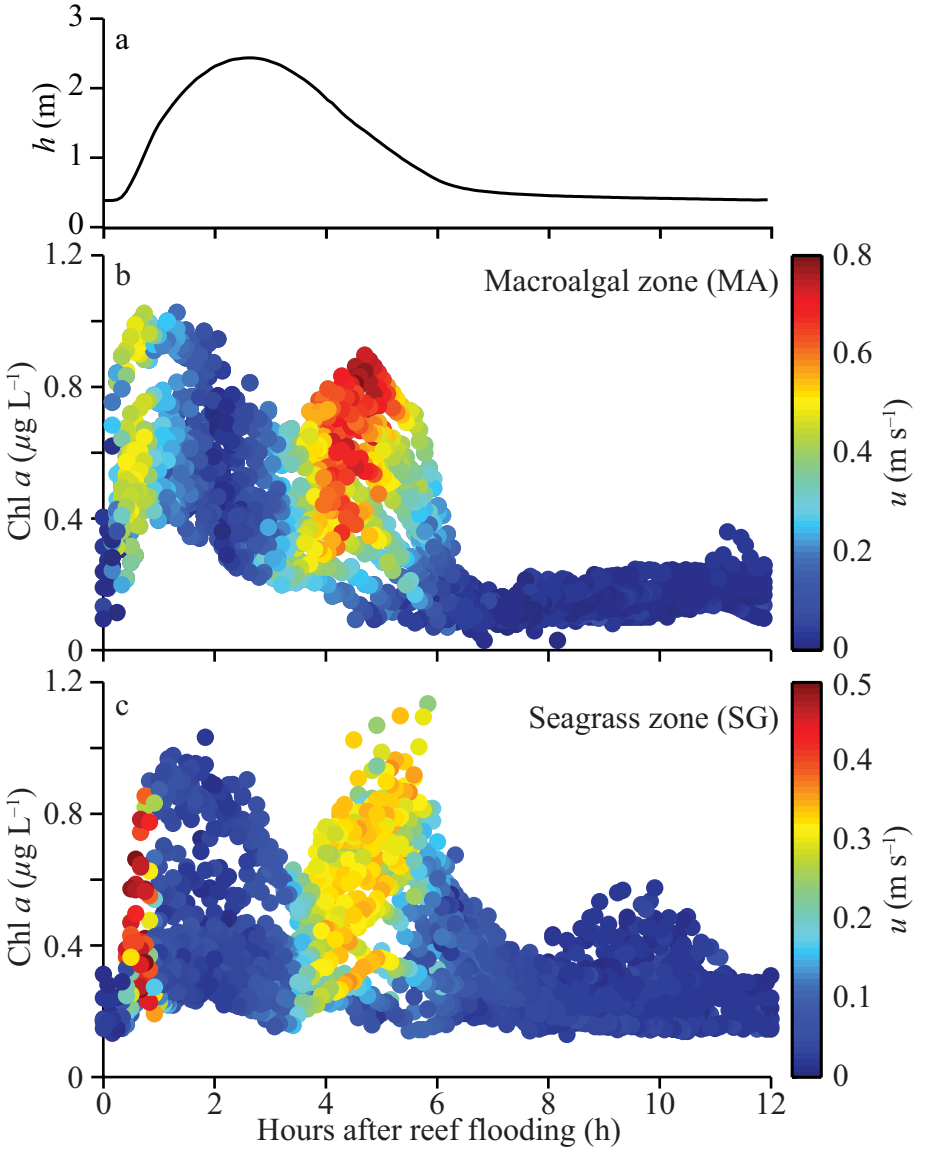

Fig. 5. Reef flat (**a**) depth *h* (tidal phase-averaged) shown with all Chl *a* measurements from fluorometers in (**b**) macroalgal and (**c**) seagrass-dominated zones shown with hour after reef flooding during the Apr field experiment. Color indicates the flow speed *u* adjacent to each fluorometer. Note that different limits are used in the color scale of each plot in order to accommodate differences in the range of flow speeds at each station.

total POC and PON to the coastal ocean during the Apr field experiment, as off-reef exports exceeded oceanic inputs (Table 4). A release of detrital material (non-phytoplanktonic) by the reef platform can be invoked to explain the difference between net uptake of POC_p and PON_p (a sink) and net export of total POC and PON. This release term is simply the sinks of POM (off-reef flow and Chl *a* uptake) less the oceanic inputs (Table 4). Detrital export is estimated to have exceeded POC_p by a factor of ~ 4 and was of similar magnitude to PON_p; thus, exported material would have a high C : N ratio ($\sim$ 15 : 1 compared to $\sim$ 7 : 1 commonly found for phytoplankton).

Discussion

Offshore Chl *a* and particulate nutrients

The southwest coast of the Kimberley is among the most pristine marine areas in the world (Halpern et al. 2008); however, water quality sampling from the three field studies reported here showed similarities between Tallon reef and reefs experiencing elevated nutrient inputs from anthropogenic sources (Schaffelke et al. 2012). Chl *a* concentrations offshore of Tallon reef (Fig. 3) were roughly double those in the macrotidal northern GBR (Brodie et al. 2007) where coastal catchments have had relatively low anthropogenic pressure (Furnas 2003; Wooldridge et al. 2006), and

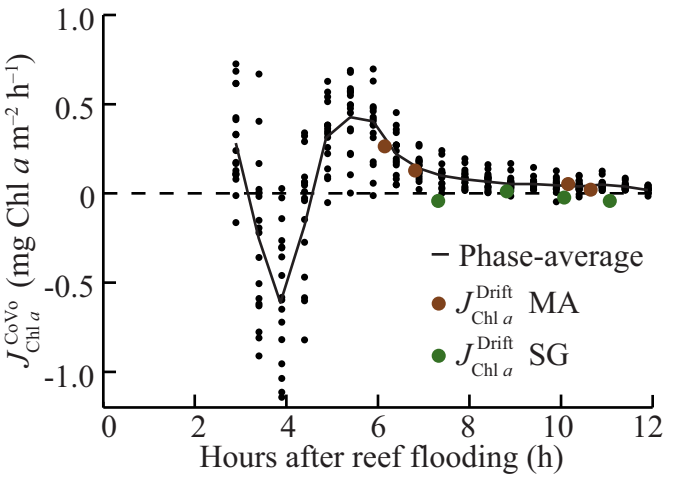

Fig. 6. All estimates of benthic flux of Chl *a* using the one-dimensional control volume technique ($J^{CoVo}_{Chl\,a}$). Positive values indicate net uptake by the reef and negative values indicate net release to overlying waters. Individual estimates (black dots) shown with tidal phase-averaged flux (line) and flux estimates from drifter releases ($J^{Drift}_{Chl\,a}$) in macroalgal (MA) and seagrass (SG)-dominated zones.

approached or exceeded the Chl *a* threshold (0.45 μg L^{-1}) used to indicate water quality favorable for high coral diversity in the GBR (De'ath and Fabricius 2010). POC concentrations measured during our study (Table 2) were similar to typical values for coral reef waters during all field experiments (Atkinson and Falter 2003; Schaffelke et al. 2012). PON concentrations were elevated (especially during Oct) relative to < 1 μM typical of reef waters (Atkinson and Falter 2003; Schaffelke et al. 2012) and were similar to nearshore reefs subject to elevated turbidity (Fabricius and Dommisse 2000). These observations further agree with other recent studies of the broader coastal Kimberley region (Thompson and Bonham 2011; Jones et al. 2014), suggesting that nearshore Kimberley reefs may naturally experience generally "meso"-trophic conditions, at least with regard to the concentration of particulate nutrients and phytoplankton.

Large seasonal differences in coastal water quality can occur in regions with a monsoonal climate as delivery of terrestrial sediment and nutrients to coastal waters occurs primarily during wet season pulsed events (Furnas 2003; Devlin and Brodie 2005), resulting in elevated coastal Chl *a* (Furnas et al. 2005; Schaffelke et al. 2012). Our study is one of the first to measure wet season Chl *a* and particulate nutrients in the coastal Kimberley (e.g., McKinnon et al. 2015*a*,*b*; Furnas and Carpenter 2016). Concentrations of Chl *a* (Fig. 3) were 50% greater by the end of the wet season (Apr), relative to dry (Oct) and mid-wet (Feb) field experiments, while POC and PON values declined (Table 2). Changes in nearshore water quality associated with terrestrial discharge during the wet season can be highly variable between events and years given that rates of terrestrial runoff are themselves highly variable (Schroeder et al. 2012). Based on monitoring data

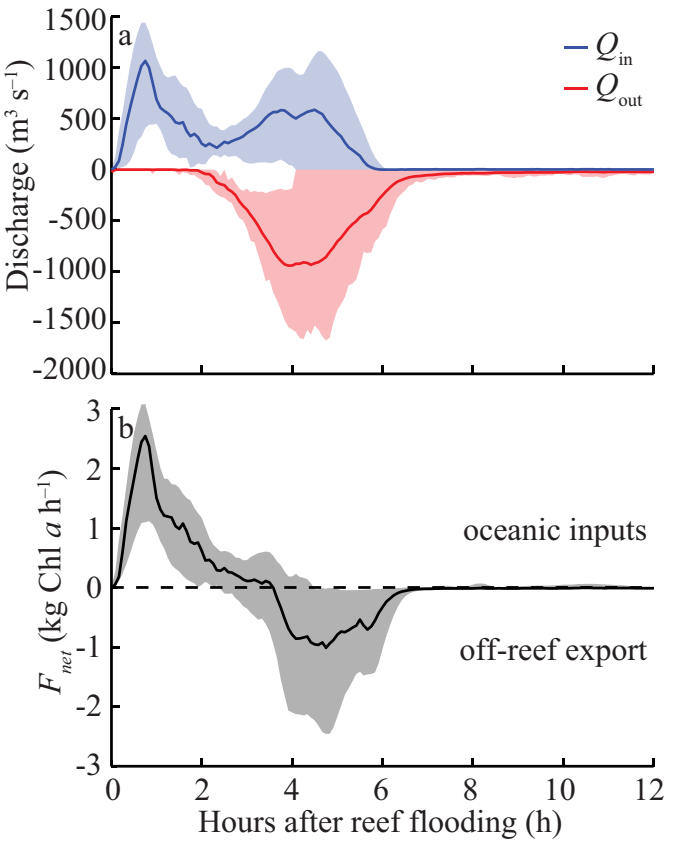

Fig. 7. Tidal phase-averaged (lines) and ranges (shaded areas) of (**a**) discharge and (**b**) net rate of Chl *a* transfer F_{net} onto (positive) and off of (negative) Tallon reef platform are shown with hours after reef flooding. Discharges are onto (Q_{in}) and off of (Q_{out}) the reef platform. [Color figure can be viewed at wileyonlinelibrary.com]

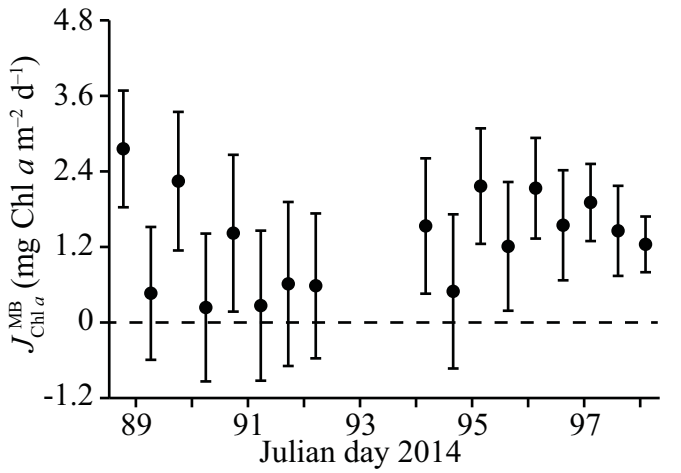

Fig. 8. Mean (± SD) vertical flux of Chl *a* over each tidal cycle determined by the mass balance technique ($J^{MB}_{Chl\,a}$) for the Apr field experiment. Positive values indicate net uptake of Chl *a* on the reef platform, while negative values indicate net release of Chl *a* to the overlying waters.

Table 3. Mean (*SD*) net benthic fluxes of Chl *a* and phytoplankton-derived particulate organic carbon (POC_p) and nitrogen (PON_p) determined by the mass balance (MB) and CoVo approaches during the Apr field experiment. Values for this study are overall means of all tidal cycle means ($n = 17$). Also shown are estimates [mean (*SE*) or range] of the same variables from previous studies of reef communities.

Study	Method	Flux (mg Chl *a* m^{-2} d^{-1})	Flux POC_p (mmol C m^{-2} d^{-1})	Flux PON_p (mmol N m^{-2} d^{-1})
This study	MB	1.31 (*0.25*)	4.0 (*1.4*)	0.95 (*0.26*)
	CoVo	1.58 (*0.18*)	4.8 (*1.7*)	1.14 (*0.31*)
Yahel et al. (2006)	Flume	0.36–1.4		1.3–5.2
Cuet et al. (2011)	MB	1.21†	3.04§	0.32
Ayukai (1995)	MB	3†	7.5*	
Genin et al. (2009)	CoVo	3.69 (*1.18*)	18.3 (*8.3*)	2.8
Wyatt et al. (2010)	Eulerian	5.67 (*0.77*)	19.6 (*2.7*)	3.43 (*0.47*)
Patten et al. (2011)	Eulerian		4–20	0.2–1.9
Monismith et al. (2010)	CoVo	9.6‡		
Fabricius and Dommisse (2000)	Eulerian	11 (*2.5*)	28.3 (*6.2*)	
Ribes and Atkinson (2007)	Flume	28–42†	70–105	7–10
Ribes et al. (2005)	Flume	31 (*2*)†	77.5 (*5*)	7.3 (*0.5*)
Yahel et al. (1998)	MB	65.6†	164	

* Includes microbial community.
† Assuming C : Chl *a* of 30.
‡ Assuming mean Chl $a = 0.2$ mg m^{-3}.
§ Assuming C : N of 9.5 based on cell data from Houlbrèque et al. (2006).

from the Fitzroy River, the largest coastal river in the west Kimberley (Fig. 1), the 2013–2014 wet season was characterized by below-average freshwater discharge (Willare station, http://water.wa.gov.au). Thus, the seasonal changes in water quality presented in this study may very well underrepresent most other years when rates of precipitation are much higher.

A substantial body of evidence has accumulated over the last 20 yr indicating that the majority of Chl *a* present in the tropical ocean water surrounding reefs (usually $\sim$ 80%) is contained within picophytoplankton defined by cell sizes < 2 μm (Charpy 2005). Studies of some coral reefs have shown that picophytoplankton can also be the largest contributor to the particulate carbon (Yahel et al. 1998; Patten et al. 2011) and nitrogen (Ribes et al. 2003) grazed by reef organisms. In our study, smaller phytoplankton ($<$ 5 μm) comprised only $\sim$ 45% of total Chl *a* in the vicinity of Tallon reef (Fig. 4a,b), which is similar to what has been found in shallow macrotidal waters such as the northern GBR and Torres Strait (Furnas and Carpenter 2016) and inshore Kimberley waters (Thompson and Bonham 2011; Jones et al. 2014). Previous work has suggested that the prevalence of larger suspended particles containing Chl *a* in the coastal Kimberley is due to particle flocculation (Jones et al. 2014), which is enhanced in the presence of suspended silt/clays (Deng et al. 2015) and strong vertical mixing (Wolanski and Spagnol 2003). Depletion of both large and small Chl *a* pools on Tallon reef coincided with significantly elevated ratios of phaeo : chl (Fig. 4c,d), which suggests that this depletion was at least partly due to grazing (Welschmeyer and Lorenzen 1985). Therefore, large particles (nanoplankton or flocculated material) could be an important component of nutrients grazed by reefs in shallow macrotidal waters. Further work incorporating flow cytometry and microscopy would help elucidate the nature of suspended particles in the coastal Kimberley.

Size-dependent deposition and resuspension of POM

Given the nature of our bulk measurements of Chl *a* and flow, it was not possible to discriminate between grazing by benthic organisms and net deposition in this study. However, we can estimate the likelihood of suspended particle deposition using the Rouse number (P), the ratio of a particle's settling velocity w_s to the shear velocity u^* as (Eisma 2012) $P = w_s/(\kappa u^*)$ where κ is the von Karman constant (0.40) and u^* is estimated from depth-averaged velocity at SG (Gruber et al. 2017); when $P \ll 1$, deposition does not occur and particle concentration is uniform with depth. Previous work has shown that POC/PON particles (and large phytoplankton) in King Sound (our "offshore" waters) were mostly in the 10–64 μm size range as (Wolanski and Gibbs 1995; Wolanski and Spagnol 2003). For this size range, w_s would be $\sim$ 0.002 cm s^{-1} (Burns and Rosa 1980), and thus negligible settling would occur ($P \ll 1$) over the entire tidal cycle. Very large POC/PON ($>$ 500 μm) with a

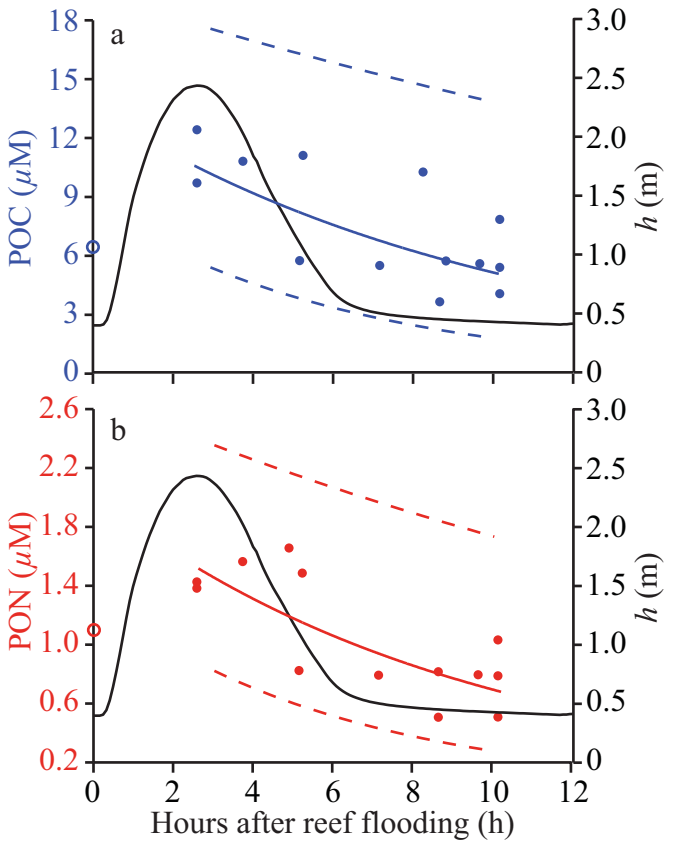

Fig. 9. Concentrations of particulate organic (**a**) carbon (POC) and (**b**) nitrogen (PON) on the reef (station Mix) during the Apr field experiment, shown as a function of hours after reef flooding. Mean tidal phase-averaged water depth *h* shown in black. Colored lines, which indicate the relationship between POC and PON with time after reef flooding ($R^2 = 0.46$ and 0.57, respectively), were used to estimate nutrient concentration in off-reef discharge during ebb tide. Dashed lines represent 95% confidence limits of the mean. Colored circles on the *x*-axis denote mean concentration offshore.

Table 4. Estimates of particulate organic carbon (POC) and nitrogen (PON) fluxes using the mass balance approach (Fig. 9; Table 3) for Tallon reef during the Apr field experiment. All values are means (SD) in mmol m^{-2} d^{-1}. Detrital release is sinks of organic material (off-reef flow and Chl *a* uptake) less the oceanic inputs.

	Sources		Sinks	
	Oceanic inputs	Detrital release	Off-reef flow	Uptake Chl *a*
POC	55.4 (*9.1*)	17.6 (*9.5*)	69 (*2.7*)	4.0 (*1.4*)
PON	9.45 (*2.21*)	1.15 (*2.25*)	9.65 (*0.34*)	0.95 (*0.26*)

much greater $w_s \sim 0.3$ cm s^{-1} (Jähmlich et al. 2002) would have a low Rouse number (< 0.7) during peak flood and ebb (0–1.5 h and 4–6 h after reef flooding, respectively). However, *P* would exceed 1 once depth-averaged flow speeds slowed to ~ 0.10 m s^{-1}, which occurred during high tide and the final 6 h of ebb (Fig. 2). Therefore, settlement of large particles likely occurs during high tide (at least temporarily) and for several hours toward the end of ebb tide after the majority of off-reef discharge has already occurred (Fig. 7). This POC/PON pool, while not grazed in suspension, would nonetheless be available for grazing by abundant benthic detritivores (such as sea cucumbers) observed on Tallon (e.g., Uthicke 1999).

With flow speeds generally high (0.3–0.4 m s^{-1}) during peak flood and ebb periods (Fig. 2b) and exceeding 0.8 m s^{-1} during spring tides, resuspension clearly plays a role in benthic fluxes of large particles on Tallon reef. In a sense, each tidal cycle serves to "flush" these larger particulates from the reef platform, as flood tide resuspends large particles that have settled during the final $\sim$ 6 h of ebb tide and "new" particulate material such as detritus generated in benthic communities during this period. This can be seen in particulate nutrient and Chl *a* concentrations during high tide and peak ebb in excess of offshore means (Figs. 5, 9) as well as negative benthic fluxes of Chl *a* during peak ebb (Fig. 6). Resuspension during peak ebb coincides with high levels of off-reef discharge (Fig. 7), so it seems likely that the majority of resuspended particles are exported off-reef each tidal cycle.

Benthic fluxes of Chl *a* and phytoplankton-derived nutrients

Net benthic fluxes of Chl *a* for Tallon reef ($\leq$ 4 mg Chl *a* m^{-2} d^{-1}) were on the lower end of previous estimates of Chl *a* uptake by reef communities, as many previous estimates are an order of magnitude larger than Tallon (Table 3). Several studies have normalized Chl *a* fluxes (*J*) to ambient Chl *a* concentrations (*C*) using the grazing rate α (in m d^{-1}) as $\alpha = J/C$, with the assumption that all Chl *a* loss is due to benthic grazing (Jones et al. 2009). Deposition of large resuspended particles occurs on Tallon reef during each tidal cycle and would be expected to obscure grazing rates. Nevertheless, if we assume that grazing was substantially greater than deposition, this would generate an α of $\sim$ 1–10 m d^{-1} for Tallon reef, which is similar to previous studies (Genin et al. 2009; Wyatt et al. 2010) but must be interpreted with caution.

Our measurements showed variability between tidal cycles, with a possible $\sim$ fortnightly periodicity (Fig. 8). Previous work on Tallon has shown that daily temperature variability (Lowe et al. 2016) and net community production (Gruber et al. 2017) can vary over a $\sim$ 15 d period driven by the differences in the phasing of the solar and semi-diurnal tidal cycle periods. In the case of Chl *a* uptake, the mechanism is more likely to be related to the volume of offshore water flooding the reef platform and flow speeds during peak ebb; these are a function of the spring-neap tidal cycle,

which also occurs at a similar fortnightly period but is not related to the solar-tidal cycle offset described above. Our results thus emphasize that short term experiments lasting a few days may greatly over- or under-estimate fluxes of particles on tide-dominated reefs. Future research in these systems should occur on scales that capture the variability in hydrodynamic processes related to the ecological or biogeochemical rates of interest.

Estimates of fluxes of carbon (POC_p, 4.0 mmol C m^{-2} d^{-1}) and nitrogen (PON_p, 0.95 mmol N m^{-2} d^{-1}) from benthic Chl *a* uptake were lower than most previous work, and were in some cases two orders of magnitude lower (Table 3). Our study may have underestimated nitrogen fluxes as we only considered particles with Chl *a*, thus neglecting the heterotrophic bacterial community, which can be abundant in coral reef waters (Ribes et al. 2003; Houlbrèque et al. 2006) and contributes disproportionately to fluxes of PON due to low C : N ratios (Patten et al. 2011). Few studies have compared the magnitude of in situ benthic fluxes of phytoplankton-derived POC and PON to reef community productivity. Studies at the organism-scale show large variability in the influence of heterotrophy on nutrient budgets (Houlbrèque and Ferrier-Pagès 2009), with some estimating that grazing can supply $\sim$ 50% and $\sim$ 30% of carbon and nitrogen requirements for coral growth (Anthony 1999), while others find that coral uptake of POC_p is a small fraction ($< 7\%$) of its gross primary production (Houlbrèque et al. 2004). Sponges, which are highly efficient filter-feeders (Reiswig 1971), can supply the majority of carbon for their respiratory demands with grazed POC (Hadas et al. 2009). Other in situ studies similarly conducted over reef scales have found grazed POC_p to be on the order of reef net primary production (Ayukai 1995; Wyatt et al. 2010) or a small fraction ($\sim$ 1%) of reef gross primary production (Ribes et al. 2005).

Assuming a photosynthetic quotient of 1 (Kinsey 1985), gross and net production for Tallon reef platform (mean of seagrass and macroalgal communities) was $\sim$ 500 mmol C m^{-2} d^{-1} and $\sim$ 30 mmol C m^{-2} d^{-1}, respectively, during the Apr experiment (Gruber et al. 2017). Thus, benthic fluxes of POC_p (Table 3) were $< 1\%$ of gross production, but were also much lower ($< 15\%$) than rates of net production, unlike many previous studies. Primary producers on the reef had relatively high tissue N and P concentrations, with mean C : N : P values of 251 : 16 : 1 found in *T. hemprichii* leaves (N. Cayabyab, unpubl.), which is well below typical values of 550 : 30 : 1 found in seagrasses and marine macroalgae (Atkinson and Smith 1983). Using tissue stoichiometry and rates of net production, nitrogen demand by primary producers could be roughly estimated as 1.9 mmol N m^{-2} d^{-1}; thus, reef PON_p fluxes (Table 3) represent roughly half of the nitrogen demand.

Net export of particulate nutrients

Unlike phytoplankton, rates of particulate nutrient uptake or release by reef communities are generally difficult to determine in situ, as concentrations of POC and PON do not typically change across the reef relative to natural variability among samples (Crossland and Barnes 1983; Houlbrèque et al. 2006); this does not necessarily indicate a lack of uptake, but rather a change in the composition of POM as water traverses the reef (Wyatt et al. 2013). To our knowledge, only one example of a reef acting as a net sink to POC (208 mmol C m^{-2} d^{-1}) and PON has been reported, which occurred in a soft coral community under elevated particulate loads (Fabricius and Dommisse 2000). A few sediment trap studies have estimated net export of POC from reefs, and generally found rates to be 4–7% of reef GPP (Delesalle et al. 1998; Hata et al. 1998, 2002); however, these studies quantified POC deposited offshore, and did not account for particulates in suspension.

In the case of Tallon reef, a water balance combined with measurable temporal changes in POC and PON concentrations allowed us to estimate the net export of particulate organic matter over a tidal cycle (Table 4). Net export (the difference between oceanic inputs and off-reef exports) of POC was 13.6 mmol C m^{-2} d^{-1}, or just $\sim$ 3% of mean reef gross primary production, while export of PON was 0.2 mmol N m^{-2} d^{-1}. These values likely underestimate total particulate export, as they only consider particles up to $\sim$ 3 mm in diameter (as determined by the diameter of water sampling tubing) and thus neglect large and rare particles, which may comprise up to two-thirds of reef POC export (Alldredge et al. 2013). Our results suggest that Tallon reef platform was both a net sink for oceanic phytoplankton and a net source of mostly detrital POC and PON to coastal waters, similar to results from a few previous field studies (Prins et al. 1996; Cuet et al. 2011; Wyatt et al. 2013). A "detrital release" term was invoked to represent the rate of (non-Chl *a*-associated) POC and PON export (17.6 mmol C and 1.15 N mmol m^{-2} d^{-1}, respectively) needed to balance POC_p and PON_p uptake (Table 4). These detrital terms are similar to what has been found for other seagrass and reef communities (25 mmol C m^{-2} d^{-1} and 8.3 mmol C m^{-2} d^{-1}, respectively), and may constitute a source of organic material for pelagic consumption just offshore of the reef (Cuet et al. 2011; Säwström et al. 2016).

In conclusion, our measurements reported here suggest that Tallon reef experiences water quality conditions similar to inshore tropical reefs worldwide that are subject to nutrient loading, yet it does not display the reef-scale net heterotrophy that has been suggested for such reefs (Fabricius 2005). Instead, uptake rates of oceanic phytoplankton on the reef were very low and the platform acted as a net source of particulate organic carbon and nitrogen to the coastal ocean. This may be related to periods of high light availability when water depth is low, as well as offshore dissolved inorganic nutrient concentrations at the upper end of reef habitats worldwide (Atkinson and Falter 2003), that enable moderate rates of reef-scale net production (Gruber et al.

2017). Deeper reefs of the coastal Kimberley (and other tide-dominated reefs with elevated POM loads) may display low rates of primary production due to reduced light availability, and thus depend more on grazing to meet the energetic needs of the reef community. This study is an important first step in identifying some of the main attributes of particle uptake on tide-dominated reefs including periods of disconnection from surrounding ocean waters, pulses of particle inputs during flood tides, and variation in fluxes within and between tidal cycles. Of course, fluxes of particulate nutrients to and from other tide-dominated reefs may differ with bathymetry, oceanic nutrient inputs, tidal range, and a whole suite of other factors. Thus, there is considerable room for future research to examine how the prevailing physics of water transport, mixing, and heating more generally control biogeochemical and ecological processes in tide-dominated reef communities.

References

Alldredge, A. L., C. A. Carlson, and R. C. Carpenter. 2013. Sources of organic carbon to coral reef flats. Oceanography **26**: 108–113. doi:10.5670/oceanog.2013.52

Anthony, K. R. N. 1999. Coral suspension feeding on fine particulate matter. J. Exp. Mar. Biol. Ecol. **232**: 85–106. doi:10.1016/S0022-0981(98)00099-9

Arar, E. J., and G. B. Collins. 1997. In vitro determination of chlorophyll *a* and pheophytin *a* in marine and freshwater algae by fluorescence, p. 1–22. Methods for the Determination of Chemical Substances in Marine and Estuarine Environmental Matrices. United States Environmental Protection Agency, Office of Research and Development, National Exposure Research Laboratory.

Atkinson, M. J., and S. V. Smith. 1983. C:N:P ratios of benthic marine plants. Limnol. Oceanogr. **28**: 568–574. doi:10.4319/lo.1983.28.3.0568

Atkinson, M. J., and J. L. Falter. 2003. Coral reefs, p. 40–64. In K. Black and G. Shimmield [eds.], Biogeochemistry of marine systems. CRC Press.

Ayukai, T. 1995. Retention of phytoplankton and planktonic microbes on coral reefs within the Great Barrier Reef, Australia. Coral Reefs **14**: 141–147. doi:10.1007/BF00367231

Bell, J. J. 2008. The functional roles of marine sponges. Estuar. Coast. Shelf Sci. **79**: 341–353. doi:10.1016/j.ecss.2008.05.002

Brodie, J., G. De'ath, M. Devlin, M. Furnas, and M. Wright. 2007. Spatial and temporal patterns of near-surface chlorophyll *a* in the Great Barrier Reef lagoon. Aust. J. Mar. Freshw. Res. **58**: 342–353. doi:10.1071/MF06236

Burns, N. M., and F. Rosa. 1980. In situ measurement of the settling velocity of organic carbon particles and 10 species of phytoplankton. Limnol. Oceanogr. **25**: 855–864. doi:10.4319/lo.1980.25.5.0855

Charpy, L. 2005. Importance of photosynthetic picoplankton in coral reef ecosystems. Vie Et Milieu **55**: 217–224.

Cloern, J. E., C. Grenz, and L. Vidergar-Lucas. 1995. An empirical model of the phytoplankton chlorophyll:carbon ratio - The conversion factor between productivity and growth rate. Limnol. Oceanogr. **40**: 1313–1321. doi:10.4319/lo.1995.40.7.1313

Crossland, C. J., and D. J. Barnes. 1983. Dissolved nutrients and organic particulates in water flowing over coral reefs at Lizard Island. Aust. J. Mar. Freshw. Res. **34**: 835–844. doi:10.1071/MF9830835

Cuet, P., and others. 2011. CNP budgets of a coral-dominated fringing reef at La Réunion, France: Coupling of oceanic phosphate and groundwater nitrate. Coral Reefs **30**: 45–55. doi:10.1007/s00338-011-0744-4

De'ath, G., and K. Fabricius. 2010. Water quality as a regional driver of coral biodiversity and macroalgae on the Great Barrier Reef. Ecol. Appl. **20**: 840–850. doi:10.1890/08-2023.1

Delesalle, B., R. Buscail, J. Carbonne, T. Courp, V. Dufour, S. Heussner, A. Monaco, and M. Schrimm. 1998. Direct measurements of carbon and carbonate export from a coral reef ecosystem (Moorea Island, French Polynesia). Coral Reefs **17**: 121–132. doi:10.1007/s003380050106

Deng, W., L. Monks, and S. Neuer. 2015. Effects of clay minerals on the aggregation and subsequent settling of marine *Synechococcus*. Limnol. Oceanogr. **60**: 805–816. doi:10.1002/lno.10059

Devlin, M. J., and J. Brodie. 2005. Terrestrial discharge into the Great Barrier Reef Lagoon: Nutrient behavior in coastal waters. Mar. Pollut. Bull. **51**: 9–22. doi:10.1016/j.marpolbul.2004.10.037

Eisma, D. 2012. Suspended matter in the aquatic environment. Springer.

Fabricius, K. E. 2005. Effects of terrestrial runoff on the ecology of corals and coral reefs: Review and synthesis. Mar. Pollut. Bull. **50**: 125–146. doi:10.1016/j.marpolbul.2004.11.028

Fabricius, K., and M. Dommisse. 2000. Depletion of suspended particulate matter over coastal reef communities dominated by zooxanthellate soft corals. Mar. Ecol. Prog. Ser. **196**: 157–167. doi:10.3354/meps196157

Furnas, M. M. J. 2003. Catchments and corals: Terrestrial runoff to the Great Barrier Reef. Australian Institute of Marine Science & CRC Reef Research Centre.

Furnas, M., A. Mitchell, M. Skuza, and J. Brodie. 2005. In the other 90%: Phytoplankton responses to enhanced nutrient availability in the Great Barrier Reef Lagoon. Mar. Pollut. Bull. **51**: 253–265. doi:10.1016/j.marpolbul.2004.11.010

Furnas, M. J., and E. J. Carpenter. 2016. Primary production in the tropical continental shelf seas bordering northern Australia. Cont. Shelf Res. **129**: 33–48. doi:10.1016/j.csr.2016.06.006

Geider, R., and J. La Roche. 2002. Redfield revisited: Variability of C:N:P in marine microalgae and its biochemical basis. Eur. J. Phycol. **37**: 1–17. doi:10.1017/S0967026201003456

Genin, A., S. G. Monismith, M. A. Reidenbach, G. Yahel, and J. R. Koseff. 2009. Intense benthic grazing of phytoplankton in a coral reef. Limnol. Oceanogr. **54**: 938–951. doi:10.4319/lo.2009.54.3.0938

Goring, D. G., and V. I. Nikora. 2002. Despiking acoustic Doppler velocimeter data. J. Hydraul. Eng. **128**: 117–126. doi:10.1061/(ASCE)0733-9429(2002)128:1(117)

Gruber, R. K., R. J. Lowe, and J. L. Falter. 2017. Metabolism of a tide-dominated reef platform subject to extreme diel temperature and oxygen variations. Limnol. Oceanogr. **62**: 1701–1717. doi:10.1002/lno.10527

Hadas, E., M. Shpigel, and M. Ilan. 2009. Particulate organic matter as a food source for a coral reef sponge. J. Exp. Biol. **212**: 3643–3650. doi:10.1242/jeb.027953

Halpern, B. S., and others. 2008. A global map of human impact on marine ecosystems. Science **319**: 948–952. doi:10.1126/science.1149345

Hata, H., A. Suzuki, T. Maruyama, N. Kurano, S. Miyachi, Y. Ikeda, and H. Kayanne. 1998. Carbon flux by suspended and sinking particles around the barrier reef of Palau, western Pacific. Limnol. Oceanogr. **43**: 1883–1893. doi:10.4319/lo.1998.43.8.1883

Hata, H., S. Kudo, H. Yamano, N. Kurano, and H. Kayanne. 2002. Organic carbon flux in Shiraho coral reef (Ishigaki Island, Japan). Mar. Ecol. Prog. Ser. **232**: 129–140. doi:10.3354/meps232129

Houlbrèque, F., E. Tambutté, C. Richard, and C. Ferrier-Pagès. 2004. Importance of a micro-diet for scleractinian corals. Mar. Ecol. Prog. Ser. **282**: 151–160. doi:10.3354/meps282151

Houlbrèque, F., B. Delesalle, J. Blanchot, Y. Montel, and C. Ferrier-Pagès. 2006. Picoplankton removal by the coral reef community of La Prevoyante, Mayotte Island. Aquat. Microb. Ecol. **44**: 59–70. doi:10.3354/ame044059

Houlbrèque, F., and C. Ferrier-Pagès. 2009. Heterotrophy in tropical scleractinian corals. Biol. Rev. **84**: 1–17. doi:10.1111/j.1469-185X.2008.00058.x

Jähmlich, S., L. C. Lund-Hansen, and T. Leipe. 2002. Enhanced settling velocities and vertical transport of particulate matter by aggregation in the benthic boundary layer. Geogr. Tidsskr. Dan. J. Geogr. **102**: 37–49. doi:10.1080/00167223.2002.10649464

Jones, N. L., J. K. Thompson, K. R. Arrigo, and S. G. Monismith. 2009. Hydrodynamic control of phytoplankton loss to the benthos in an estuarine environment. Limnol. Oceanogr. **54**: 952–969. doi:10.4319/lo.2009.54.3.0952

Jones, N. L., N. L. Patten, D. L. Krikke, R. J. Lowe, A. M. Waite, and G. N. Ivey. 2014. Biophysical characteristics of a morphologically-complex macrotidal tropical coastal system during a dry season. Estuar. Coast. Shelf Sci. **149**: 96–108. doi:10.1016/j.ecss.2014.07.018

Kinsey, D. W. 1985. Metabolism, calcification and carbon production. I. System level studies, p. 503–542. Proceedings of the 5th International Coral Reef Congress, Tahiti, 27 May–1 June 1985.

Kordi, M. N., and M. O'Leary. 2016. Geomorphic classification of coral reefs in the north western Australian shelf. Reg. Stud. Mar. Sci. **7**: 100–110. doi:10.1016/j.rsma.2016.05.012

Kowalik, Z. 2004. Tide distribution and tapping into tidal energy. Oceanologia **46**: 291–331.

Lehrter, J. C., and J. Cebrian. 2010. Uncertainty propagation in an ecosystem nutrient budget. Ecol. Appl. **20**: 508–524. doi:10.1890/08-2222.1

Lowe, R. J., and J. L. Falter. 2015. Oceanic forcing of coral reefs. Annu. Rev. Mar. Sci. **7**: 43–66. doi:10.1146/annurev-marine-010814-015834

Lowe, R. J., A. S. Leon, G. Symonds, J. L. Falter, and R. Gruber. 2015. The intertidal hydraulics of tide-dominated reef platforms. J. Geophys. Res. Oceans **120**: 4845–4868. doi:10.1002/2015JC010701

Lowe, R. J., X. Pivan, J. Falter, G. Symonds, and R. Gruber. 2016. Rising sea levels will reduce extreme temperature variations in tide-dominated reef habitats. Sci. Adv. **2**: e1600825. doi:10.1126/sciadv.1600825

McKinnon, A. D., J. Doyle, S. Duggan, M. Logan, C. Lønborg, and R. Brinkman. 2015*a*. Zooplankton growth, respiration and grazing on the Australian margins of the tropical Indian and Pacific Oceans. PLoS One **10**: e0140012. doi:10.1371/journal.pone.0140012

McKinnon, A. D., S. Duggan, D. Holliday, and R. Brinkman. 2015*b*. Plankton community structure and connectivity in the Kimberley-Browse region of NW Australia. Estuar. Coast. Shelf Sci. **153**: 156–167. doi:10.1016/j.ecss. 2014.11.006

Menzel, D. W., and N. Corwin. 1965. The measurement of total phosphorus in seawater based on the liberation of organically bound fractions by persulfate oxidation. Limnol. Oceanogr. **10**: 280–282. doi:10.4319/lo.1965. 10.2.0280

Monismith, S. 2007. Hydrodynamics of coral reefs. Annu. Rev. Fluid Mech. **39**: 37–55. doi:10.1146/annurev.fluid.38.050304.092125

Monismith, S. G., and others. 2010. Flow effects on benthic grazing on phytoplankton by a Caribbean reef. Limnol. Oceanogr. **55**: 1881–1892. doi:10.4319/lo.2010.55.5.1881

Parsons, T. R., M. Takahashi, and B. Hargrave. 1984. Biological oceanographic processes. Pergamon Press.

Patten, N. L., A. S. J. Wyatt, R. J. Lowe, and A. M. Waite. 2011. Uptake of picophytoplankton, bacterioplankton and virioplankton by a fringing coral reef community (Ningaloo Reef, Australia). Coral Reefs **30**: 555–567. doi:10.1007/s00338-011-0777-8

Prins, T. C., A. C. Smaal, A. J. Pouwer, and N. Dankers. 1996. Filtration and resuspension of particulate matter and phytoplankton on an intertidal mussel bed in the Oosterschelde estuary (SW Netherlands). Mar. Ecol. Prog. Ser. **142**: 121–134. doi:10.3354/meps142121

Reiswig, H. M. 1971. Particle feeding in natural populations of three marine demosponges. Biol. Bull. **141**: 568–591. doi:10.2307/1540270

Ribes, M., R. Coma, M. J. Atkinson, and R. A. Kinzie. 2003. Particle removal by coral reef communities: Picoplankton

is a major source of nitrogen. Mar. Ecol. Prog. Ser. **257**: 13–23. doi:10.3354/meps257013

Ribes, M., R. Coma, M. J. Atkinson, and R. A. Kinzie. 2005. Sponges and ascidians control removal of particulate organic nitrogen from coral reef water. Limnol. Oceanogr. **50**: 1480–1489. doi:10.4319/lo.2005.50.5.1480

Ribes, M., and M. J. Atkinson. 2007. Effects of water velocity on picoplankton uptake by coral reef communities. Coral Reefs **26**: 413–421. doi:10.1007/s00338-007-0211-4

Richter, C., M. Wunsch, M. Rasheed, I. Kotter, and M. I. Badran. 2001. Endoscopic exploration of Red Sea coral reefs reveals dense populations of cavity-dwelling sponges. Nature **413**: 726–730. doi:10.1038/35099547

Säwström, C., and others. 2016. Coastal connectivity and spatial subsidy from a microbial perspective. Ecol. Evol. **6**: 6662–6671. doi:10.1002/ece3.2408

Schaffelke, B., J. Carleton, M. Skuza, I. Zagorskis, and M. J. Furnas. 2012. Water quality in the inshore Great Barrier Reef lagoon: Implications for long-term monitoring and management. Mar. Pollut. Bull. **65**: 249–260. doi:10.1016/j.marpolbul.2011.10.031

Schroeder, T., M. J. Devlin, V. E. Brando, A. G. Dekker, J. E. Brodie, L. A. Clementson, and L. McKinna. 2012. Inter-annual variability of wet season freshwater plume extent into the Great Barrier Reef lagoon based on satellite coastal ocean colour observations. Mar. Pollut. Bull. **65**: 210–223. doi:10.1016/j.marpolbul.2012.02.022

Thompson, P. A., and P. Bonham. 2011. New insights into the Kimberley phytoplankton and their ecology. J. R. Soc. West. Aust. **94**: 161–170.

Uthicke, S. 1999. Sediment bioturbation and impact of feeding activity of *Holothuria* (*Halodeima*) *atra* and *Stichopus chloronotus*, two sediment feeding holothurians, at Lizard Island, Great Barrier Reef. Bull. Mar. Sci. **64**: 129–141.

Volkman, J. K., and E. Tanoue. 2002. Chemical and biological studies of particulate organic matter in the ocean. J. Oceanogr. **58**: 265–279. doi:10.1023/A:1015809708632

Wells, F., J. R. Hanley, and D. I. Walker. 1995. Marine biological survey of the southern Kimberley, Western Australia, p. 152. Western Australian Museum.

Welschmeyer, N. A., and C. J. Lorenzen. 1985. Chlorophyll budgets: Zooplankton grazing and phytoplankton growth in a temperate fjord and the Central Pacific Gyres. Limnol. Oceanogr. **30**: 1–21. doi:10.4319/lo.1985.30.1.0001

Wolanski, E., and R. J. Gibbs. 1995. Flocculation of suspended sediment in the Fly River Estuary, Papua New Guinea. J. Coast Res. **11**: 754–762.

Wolanski, E., and S. Spagnol. 2003. Dynamics of the turbidity maximum in King Sound, tropical Western Australia. Estuar. Coast. Shelf Sci. **56**: 877–890. doi:10.1016/S0272-7714(02)00214-7

Wooldridge, S., J. Brodie, and M. Furnas. 2006. Exposure of inner-shelf reefs to nutrient enriched runoff entering the Great Barrier Reef Lagoon: Post-European changes and the design of water quality targets. Mar. Pollut. Bull. **52**: 1467–1479. doi:10.1016/j.marpolbul.2006.05.009

Wyatt, A. S. J., R. J. Lowe, S. Humphries, and A. M. Waite. 2010. Particulate nutrient fluxes over a fringing coral reef: Relevant scales of phytoplankton production and mechanisms of supply. Mar. Ecol. Prog. Ser. **405**: 113–130. doi:10.3354/meps08508

Wyatt, A. S. J., J. L. Falter, R. J. Lowe, S. Humphries, and A. M. Waite. 2012. Oceanographic forcing of nutrient uptake and release over a fringing coral reef. Limnol. Oceanogr. **57**: 401–419. doi:10.4319/lo.2012.57.2.0401

Wyatt, A. S., R. J. Lowe, S. Humphries, and A. M. Waite. 2013. Particulate nutrient fluxes over a fringing coral reef: Source-sink dynamics inferred from carbon to nitrogen ratios and stable isotopes. Limnol. Oceanogr. **58**: 409–427. doi:10.4319/lo.2013.58.1.0409

Yahel, G., A. F. Post, K. Fabricius, D. Marie, D. Vaulot, and A. Genin. 1998. Phytoplankton distribution and grazing near coral reefs. Oceanography **43**: 551–563. doi:10.4319/lo.1998.43.4.0551

Yahel, G., T. Zalogin, R. Yahel, and A. Genin. 2006. Phytoplankton grazing by epi- and infauna inhabiting exposed rocks in coral reefs. Coral Reefs **25**: 153–163. doi:10.1007/s00338-005-0075-4

Yentsch, C. S., and R. F. Vaccaro. 1958. Phytoplankton nitrogen in the oceans. Limnol. Oceanogr. **3**: 443–448. doi:10.4319/lo.1958.3.4.0443

Acknowledgments

Our team would like to acknowledge the Bardi Jawi, the Traditional Owners both past and present, who continue to care for this country. Thanks to the Bardi Jawi Rangers and staff of the Kimberley Marine Research Station for their help and local knowledge on three field trips. We are grateful for field assistance provided by Michael Cuttler, Jordan Iles, Miela Kolomaznik, and Leonardo Ruiz-Montoya. Comments by two anonymous reviewers substantially clarified and improved earlier drafts of this paper. This work was funded by the Western Australian Marine Science Institution's Kimberley Marine Research Program (Project 2.2.3), an Australian Research Council's Future Fellowship (FT110100201) to RJL, and the ARC Centre of Excellence for Coral Reef Studies (CE140100020).

Conflict of Interest

None declared.

Submitted 14 March 2017
Revised 15 September 2017; 15 December 2017
Accepted 17 January 2018

Associate editor: James Leichter